Supplement of Biogeosciences, 22, 3681–3697, 2025
https://doi.org/10.5194/bg-22-3681-2025-supplement

Biogeosciences
Open Access

Supplement of

Coccolithophore abundance and production and their impacts on particulate inorganic carbon cycling in the western North Pacific

Yuye Han et al.

Correspondence to: Zhimian Cao (zmcao@xmu.edu.cn) and Minhan Dai (mdai@xmu.edu.cn)

S1 Supplementary Figures

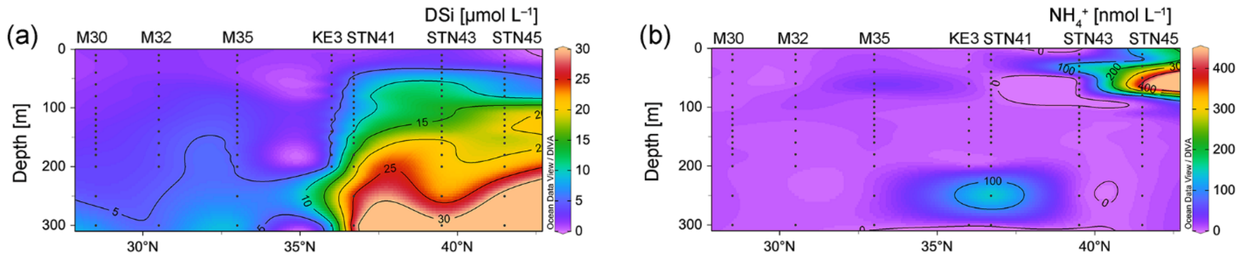

Fig. S1. Vertical depth distributions of (a) dissolved silicate (DSi) and (b) ammonium (NH_4^+) concentrations in the upper 300 m of the water column (Schlitzer Reiner, Ocean Data View, https://odv.awi.de/, last access: 23 November 2023, 2020).

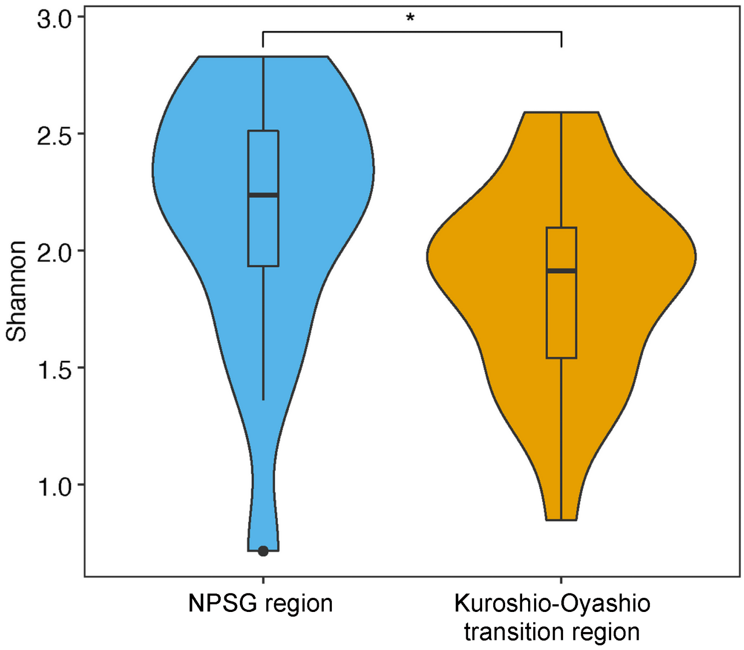

Fig. S2. Comparison of the Shannon diversity index of the coccolithophore phytoplankton community between the North Pacific Subtropical Gyre (NPSG) region and the Kuroshio-Oyashio transition region. * represents a statistical significance of $p < 0.05$, which indicates that the coccolithophore assemblage diversity in the NPSG region was significantly higher than in the Kuroshio-Oyashio transition region.

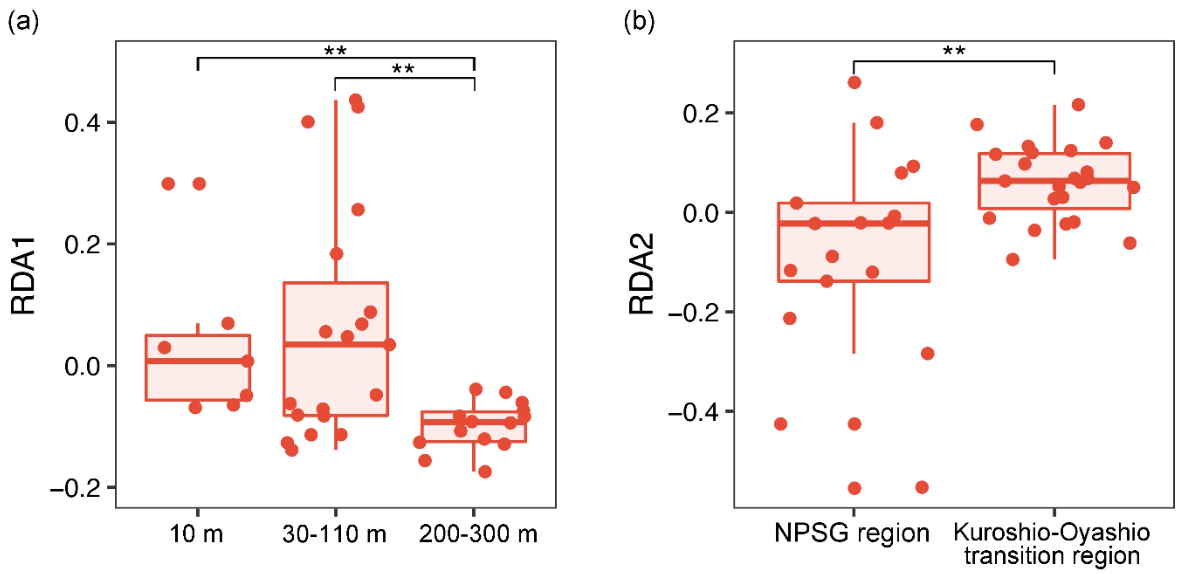

Fig. S3. Relationship (a) between the redundancy analysis (RDA)1 axis and different depths and (b) between the RDA2 axis and the two ocean regions targeted in this study. ** indicates a statistical significance of $p < 0.01$; NPSG represents the North Pacific Subtropical Gyre.

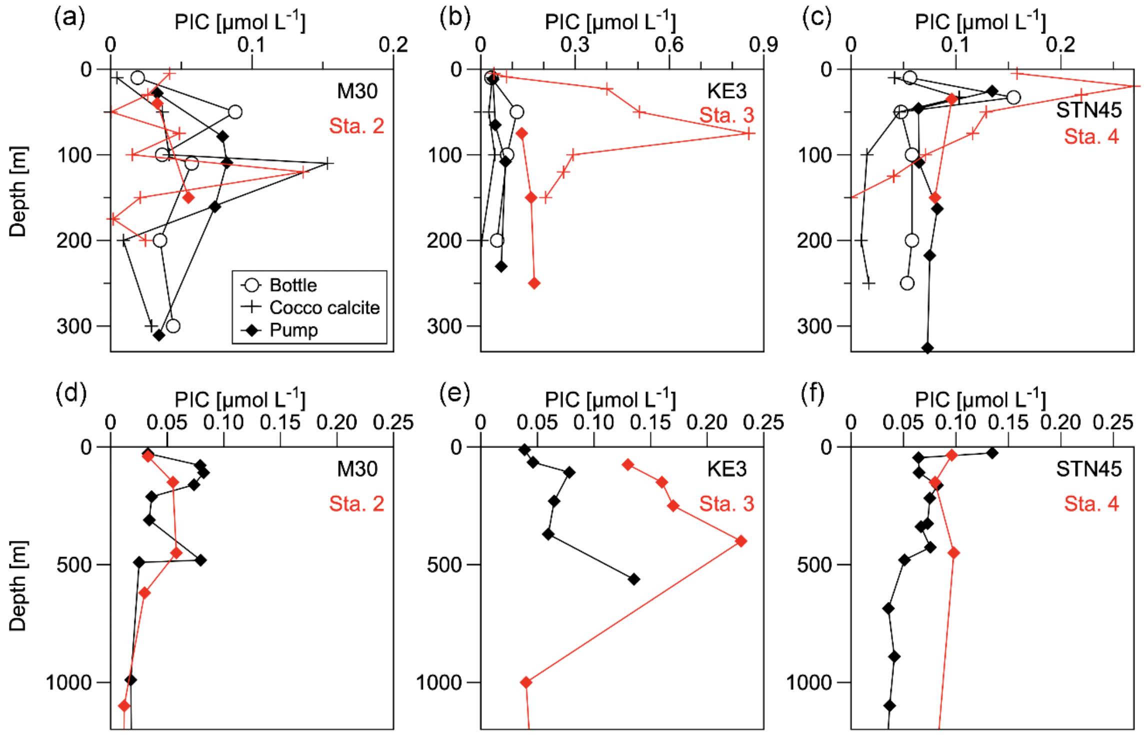

Fig. S4. Vertical depth profiles of particulate inorganic carbon (PIC) concentrations from Niskin bottle-sampling, coccolithophore (Cocco) calcite and PIC concentrations from in-situ pump-sampling at stations M30 (28.5°N, 155°E), KE3 (36°N, 155°E) and STN45 (41.5°N, 155°E) (see Fig. 1) in the (a–c) upper 350 m and (d–f) 1,200 m of the water-column, respectively. Red symbols are data from Sta.2 (27.73°N, 155.25°W), Sta.3 (35.26°N, 150.98°W) and Sta.4 (41.75°N, 148.25°W) investigated during the CDisK-IV cruise (Dong et al., 2019; Ziveri et al., 2023).

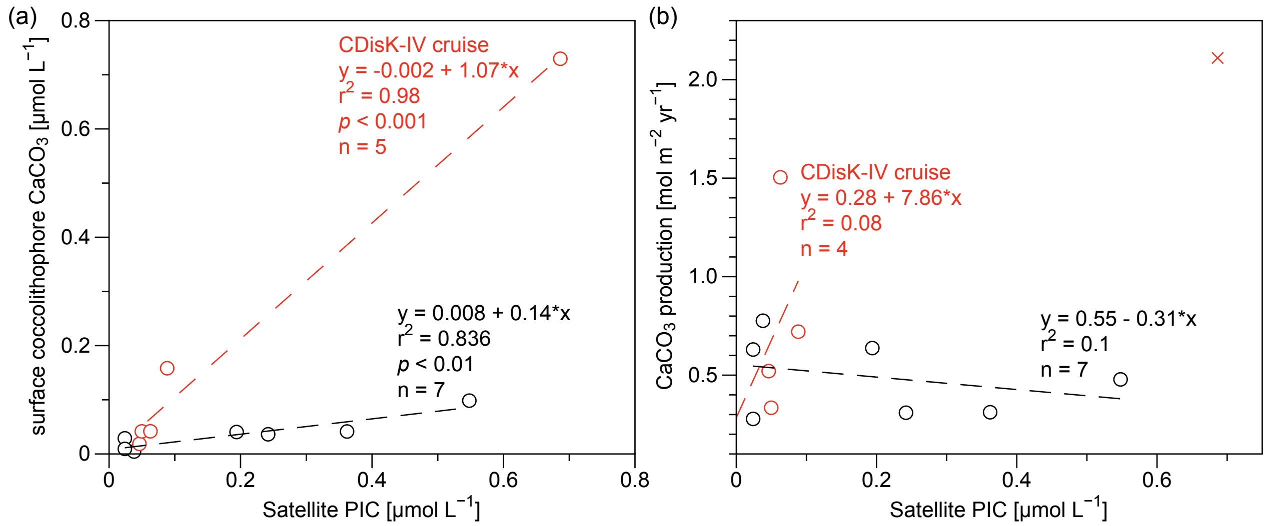

Fig. S5. Scatter plots showing relationships (a) between surface coccolithophore calcite concentrations and satellite-derived particulate inorganic carbon (PIC) concentrations; (b) between coccolithophore $CaCO_3$ production rate (not seasonal corrected) in the euphotic zone and satellite-derived PIC concentrations. The red symbols denote data from the CDisK-IV cruise with the cross representing an outlier excluded from the linear regression analysis, and the $CaCO_3$ production rate here only includes contributions from coccolithophores (Ziveri et al., 2023).

S2 Supplementary Tables

Table S1. Location of the seven sampling stations and their euphotic zone depth during the NORC2022-306 cruise. Stations M30, M32 and M35 were in the North Pacific Subtropical Gyre, and the remaining stations were in the Kuroshio-Oyashio transition region.

Station	Latitude (°N)	Longitude (°E)	Euphotic zone depth (m)
M30	28.5	155	219
M32	30.5	155	137
M35	33.0	155	158
KE3	36.0	155	142
STN41	36.7	155	130
STN43	39.5	155	108
STN45	41.5	155	103

Table S2. Coccolith mass estimates of the main coccolithophore species using morphometrics. The species-specific K_s values used were from Young and Ziveri (2000) and Jin et al. (2016). C_N, the number of coccoliths per cell, was obtained from Yang and Wei (2003) and Boeckel and Baumann (2008).

Species	Length (μm)	K_s	Mass $CaCO_3$ (pg)	C_N
Emiliania huxleyi	3.48±0.22	0.02	2.28	24
Gephyrocapsa ericsonii	2.04±0.21	0.05	1.15	15
Gephyrocapsa oceanica	4.87±0.52	0.05	15.59	23
Discosphaera tubifera	3.67±0.34	0.07	9.34	47
Umbellosphaera tenuis	5.72±0.74	0.015	7.58	25
Umbellosphaera irregularis	5.72±0.74	0.015	7.58	26
Syracosphaera molischii	3.01±0.41	0.03	2.21	38
holo-coccolithophores	4.03±0.25	0.03	5.30	70
Algirosphaera robusta	2.83±0.29	0.06	3.67	32
Florisphaera profunda	3.69±0.71	0.04	5.43	62
Calcidiscus leptoporus	7.35±1.03	0.08	85.77	29
Oolithotus fragilis	7.35±1.03	0.07	75.05	32
Umbilicosphaera sibogae	4.85±0.43	0.05	15.40	68
Helicosphaera carteri	9.87±0.95	0.05	129.80	21

Supplementary References

Boeckel, B. and Baumann, K.-H.: Vertical and lateral variations in coccolithophore community structure across the subtropical frontal zone in the South Atlantic Ocean, Marine micropaleontol, 67, 255-273, https://doi.org/10.1016/j.marmicro.2008.01.014, 2008.

Dong, S., Berelson, W. M., Rollins, N. E., Subhas, A. V., Naviaux, J. D., Celestian, A. J., Liu, X., Turaga, N., Kemnitz, N. J., and Byrne, R. H.: Aragonite dissolution kinetics and calcite/aragonite ratios in sinking and suspended particles in the North Pacific, Earth Planet Sc Lett, 515, 1-12, https://doi.org/10.1016/j.epsl.2019.03.016, 2019.

Jin, X., Liu, C., Poulton, A. J., Dai, M., and Guo, X.: Coccolithophore responses to environmental variability in the South China Sea: species composition and calcite content, Biogeosciences, 13, 4843-4861, https://doi.org/10.5194/bg-13-4843-2016, 2016.

Schlitzer, R.: Ocean Data View, https://odv.awi.de (last access: 23 November 2023), 2020.

Yang, T. N. and Wei, K. Y.: How many coccoliths are there in a coccosphere of the extant coccolithophorids? A compilation, Br. Phycol. J, 26, 67-80, https://doi.org/10.58998/jnr2275, 2003.

Young, J. R. and Ziveri, P.: Calculation of coccolith volume and it use in calibration of carbonate flux estimates, Deep sea research II, 47, 1679-1700, https://doi.org/10.1016/s0967-0645(00)00003-5, 2000.

Ziveri, P., Gray, W. R., Anglada-Ortiz, G., Manno, C., Grelaud, M., Incarbona, A., Rae, J. W. B., Subhas, A. V., Pallacks, S., and White, A.: Pelagic calcium carbonate production and shallow dissolution in the North Pacific Ocean, Nat Commun, 14, 805, https://doi.org/10.1038/s41467-023-36177-w, 2023.